Conversion of methanol to hydrocarbons over zeolite ZSM-23: Exceptional effects of particle size on catalyst lifetime

A. Molino,a D. Rojo-Gama,a K. A. Lukaszuk,a K. P. Lillerud,a U. Olsbye,a S. Bordiga,a,c S. Svelle,*a and P. Beato*b

a. Center for Materials Science and Nanotechnology, Department of Chemistry, University of Oslo, P.O. Box 1033 Blindern, N-0315 Oslo, Norway

b. . Haldor Topsøe A/S, Nymøllevej 55, DK-2800 Lyngby, Denmark

c. Department of Chemistry, NIS and INSTM Reference Centers, University of Turin, via Quarello 15, I-10135 Turin, Italy

A variety of synthetic procedures have been used to obtain zeolite ZSM-23 (MTT) catalysts with crystallite sizes ranging from the micrometer to nanometer scale. When the acidic zeolite is used as catalyst for the Methanol to hydrocarbons (MTH) reaction, the catalytic lifetime is dramatically influenced by the crystallite shape and size.

The Methanol to Hydrocarbon reaction is an important process in a chain of processes to convert carbon rich feedstocks such as coal, natural gas, or biomass into hydrocarbon species such as light alkenes or gasoline fuel over porous acidic zeolite and zeotype catalysts. Because the reaction occurs within pores of molecular dimensions, the product selectivity is highly sensitive to the size and arrangement of the channel system; this is known as product shape selectivity. Of particular interest are medium pore zeolites (pore circumference defined by 10 oxygens), such as the commercially employed ZSM-5 catalyst (10-ring intersecting channels that form a three dimensional porous network). This catalyst is used in the Mobil Methanol to Gasoline (MTG)1 and Topsøe Improved Gasoline Synthesis TIGAS2 processes and shows a high selectivity towards an aromatics rich gasoline range C5-C6+ product.

Recently, it has been demonstrated that some 10-ring zeolites with non-intersecting, one dimensional channels, such as ZSM-22 (TON) and ZSM-23 (MTT) also show a high selectivity towards C5-C6+, but with a very low amount of aromatics3. Such a product could be used as "clean gasoline", similar to alkylate4 and isomerate5. In the absence of channel intersections, aromatics formation and especially reactivity is limited6, but rapid deactivation caused by pore blocking is an issue because of the one-dimensional pore system. However, the role of the catalysis at the pore mouth for both ZSM-22 and ZSM-23 is still argued6,7.

The one dimensional medium pore zeolite ZSM-23 was first synthesized by Rubin8. It is a high silica framework, belonging to the MTT topology. As many other unidirectional materials ZSM-23 tends to grow with a needle-like shape morphology3 with high aspect ratio, where the channel direction is parallel to the longest dimension of the needle9.

It is known that the zeolite crystallite size may influence the catalysts activity and selectivity, and in particular the catalyst lifetime. For example, the conversion of methanol10, ethanol, and 2-propanol11 to hydrocarbons has been studied on the SAPO-34 and SAPO-3512 zeotype catalyst, and

an increase of one order of magnitude in the catalytic lifetime13 was seen for the nano-sized SAPO-34 compared to the micrometric-sized. Moreover, for ZSM-5 a similar trend was observed13 for the MTH reaction. Khare et al.14 have highlighted how increasing the particle size may lead to higher selectivity towards light alkenes due to a longer intra-crystalline residence time of key intermediates in the MTH reaction over ZSM-5. Of particular relevance to this study is the work of Wang et al.15 who employed ball milling to produce nanosized ZSM-22 with substantially improved MTH lifetime.

In this work, a series of zeolite ZSM-23 (MTT) catalysts with different particle size and morphology have been prepared using direct synthesis and applied as catalysts for the conversion of methanol into hydrocarbons. A profound effect of particle size on lifetime is demonstrated. The best catalyst does nearly two orders of magnitude more turnovers compared to previous reports for the same and comparable topologies. This might pave the way for commercial (fixed bed) applications, which previously has been unrealistic due to short lifetimes.

Zeolite catalyst synthesis

ZSM-23 catalysts with different crystallite sizes were prepared by modifying synthetic procedures described in literature. The reported gel compositions were adjusted to obtain products with similar Si/Al ratios; in the range 20-40. Key information is presented in Table 1, and the exact details of the synthesis procedures are presented in the Supplementary Information. The catalysts are labelled according to the structure directing agent (SDA) employed: ZSM-23 DMF for N,N-dimethylformamide16,17, ZSM-23 Pyrr for Pyrrolidine9, ZSM-23 iPA for isopropylamine9, ZSM-23 T/HMPD for a molar mixture of 70% N1,N1,N3,N3-tetramethylpropane-1,3-diamine (TMPD) and 30% N1,N1,N3,N3,2,2-hexamethylpropane-1,3-diamine (HMPD) 18, ZSM-23 C7 diquat as heptamethonium bromide (N,N,N,N',N',N'-hexamethylheptane-1,7-diaminium dibromide)19–22.

As a representative example, the synthesis with isopropylamine (iPA) was carried out as follows:

-0.064 g of $NaAlO_2$ and 0.093 g of $Al(NO_3)_3 \cdot 18H_2O$ were mixed in a Teflon liner under stirring in 18 g of H_2O until obtaining a clear solution

-2 g of fumed silica (Aldrich) was added slowly while stirring, resulting in the formation of a viscous mixture.

-5.5 ml of isopropylamine was added to this mixture.

The gel was stirred with a magnet for 3h at room temperature. Then, the Teflon liner was placed in a stainless steel autoclave. The crystallization was performed in a tumbling oven (rotation speed 30 rpm) which was preheated to 160 °C.

Table 1 Precursor gel molar batch composition of the different samples of ZSM-23

Catalyst	SiO_2	Al_2O_3	H_2O	Na_2O	SDA[a]	Si source	Al source	SDA type	Time (h)	t °C
ZSM-23 DMF	1	0,014	29,5	0,36	0,55	Colloidal SiO_2	$Al_2(SO_4)_3$	DMF	94	185
ZSM-23 Pyrr	1	0,03	45,5	0,20	0,45 [a]	Fumed SiO_2	$Al(NO_3)_3$	Pyrrolidine	66	180
ZSM-23 iPA	1	0,012	26,7	0,046	2	Fumed SiO_2	$NaAlO_2$	Isopropylamine	92	160
ZSM-23 H/TMPD	1	0,025	31	0,06	1	Colloidal SiO_2	$NaAlO_2$	30% HMPD/70% TMPD	160	160
ZSM-23 C7 diquat	1	0,03	40	0,16	0,15	Fumed SiO_2	$Al(NO_3)_3$	Heptamethoniumbromide	335	160

After 92 h, the autoclave was quenched in cold water and the product was collected by filtration and washed several times with distilled water. The product was then dried overnight at 80 °C. Organic compounds trapped in the pores were removed by calcination in a muffle furnace at 550 °C (6 h heating from RT, 8 h hold time). The sample was then ion exchanged 3 times with a 1 M solution of NH4NO3 at 80 °C for 3-5 h. The sample in the ammonium form was then calcined again with the same condition as before.

Characterization methods

Powder X-Ray diffraction (PXRD) patterns were acquired using a Bruker D8 Discover diffractometer equipped with a Cu Kα source, germanium crystal monochromator (022 plane) and a LynxEye silicon detector.

Nitrogen adsorption measurements were done volumetrically at 77K in a BELSORP-Mini II instrument. The samples were evacuated at 80 °C for 1 h and at 250 °C for 3 h before the adsorption measurement. The surface area was calculated using the BET method23 in the range of validity for microporous materials24. The micropore volume was calculated using the t-plot method (see Supplementary Information).

Scanning electron microscopy (SEM) was carried out with a Hitachi SU8200 instrument with a Cold Field Emission gun source, using a voltage of 3 kV. The uncoated sample in the powder form was glued on the holder with carbon tape. The zeolite elementary composition was measured by Energy Dispersive X-ray Spectroscopy (EDX) with an accelerating voltage of 8 kV on a sample pressed to a pellet.

The conversion of methanol to hydrocarbons was performed in a continuous flow U-shaped fix-bed reactor (i.d. of 10 mm). Prior to reactions, catalysts were heated from room temperature to 550 °C under a flow of 10 mL/min of pure He. After reaching the pretreatment temperature, the flowing gas was switched to pure O2 and kept for 1 hour to calcine the catalysts in-situ to remove all adsorbed species. After the pre-treatment, the reactor was cooled down under a flow of pure He to the temperature applied for the reaction (400 °C).

The methanol to hydrocarbon reaction was carried out at atmospheric pressure and 400 °C. 100 mg of catalyst was used (sieve fraction 250 to 420 µm). A He flow of 19.5 mL min-1 was bubbled through a saturator filled with MeOH (BDH Laboratory, purity >99.8 %) at a temperature of 20 °C, giving rise to a methanol partial pressure of 130 mbar. The resulting weight hourly space velocity (WHSV) was 2 gMeOH gcatalyst-1 h-1.

The reaction products were analysed using an online Agilent 6890A gas chromatograph equipped with an SPB-5 capillary column (length 60 m, 0.530 mm i.d., stationary phase thickness of 5 µm) and a flame ionization detector (FID).

Methanol conversion, product selectivity and product yield were obtained by the integration of the areas from the GC-FID chromatogram. Both, methanol (MeOH) and dimethyl ether (DME) were considered to be reactants and the rest of compounds detected in the GC as products of reaction. Measured response factors were used for MeOH and DME, whereas the response was considered proportional to the number of carbon atoms in the molecule for the hydrocarbon products.

Results – catalyst characterization

Characterization data are presented in Figure 1 (SEM and XRD) and Table 2. As is evident from these data, by using different structure directing agents, it has been possible to synthesize a series of ZSM-23 catalysts with similar Si/Al ratio (and thus acid site density, Table 2) in the range of 20-30, but with very different particle size and morphology. It has previously been demonstrated that the MTT channels strongly prefer to be aligned with the longest direction of the crystals9 This has also been verified using electron imaging and diffraction for some of the samples studied here (not shown). Thus, we are particularly interested in the longest particle dimension, as this can reasonable be related to the catalyst performance in a unidirectional system6,15 This information has been

extracted from SEM and is summarized in Table 2, and the catalysts may be ranked by size accordingly: ZSM-23 DMF > ZSM-23 iPA > ZSM-23 Pyrr > ZSM-23 H/TMPD >> ZSM-23 C7 Diquat.

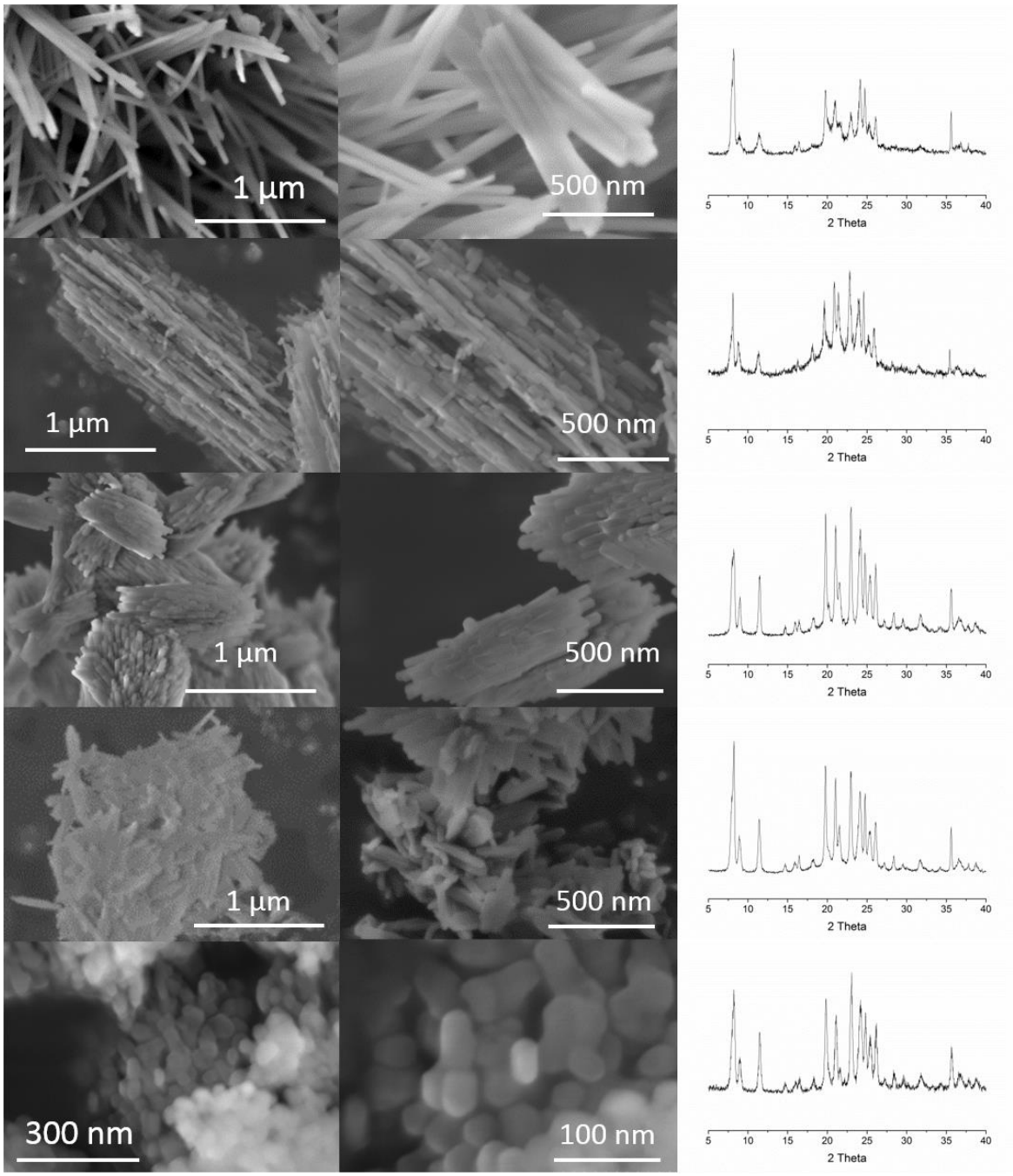

Fig. 1 Low resolution scanning electron images (left column), high resolution images (middle column) and powder X-ray diffractograms for five ZSM-23 catalysts. From top to bottom: ZSM-23 DMF, ZSM-23 pyrrolidine, ZSM-23 H/TMPD, ZSM-23 isopropylamine, ZSM-23 C7 diquat

The LeBail refined powder X-ray diffractograms (see Supporting Information) show that the use of isopropylamine, the mixed templating agent H/TMPD, or the diquaternary templating agent gives a highly crystalline pure phase of ZSM-23 (MTT). The use of DMF and pyrrolidine gives less sharp reflections around 22°. This might be due to the presence of amorphous siliceous phase (in particular for the DMF sample, which displays a low surface area, Table 2). Alternatively, the broader reflections might be caused by be the presence of a high number of stacking faults, which can generate an intergrowth phase MTT/TON (SSZ-54), which has been described for the synthesis of high aluminium containing phases in the presence of dimethylamine25,26. Obviously, dimethylamine will be produced by hydrolysis of DMF at the basic conditions used here.

Table 2 Characterization of the ZSM-23 samples

	BET surface area (m^2/g)	Si/Al (EDX)	Crystal length in nm (SEM)	Conversion capacity (g_{MeOH} / g_{cat})
ZSM-23 DMF	150	26	500-1000	1.1
ZSM-23 Pyrrolidine	271	23	120	12
ZSM-23 iPA	264	28	160	5.7
ZSM-23 H/TMPD	281	18	110	7.7
ZSM-23 C7 Diquat	276	27	40	70

Many aspects influence the outcome of these synthesis protocols, and it is not straightforward to produce materials with similar compositions. Ernst et al22 have studied the crystallization of ZSM-23 and suggested that a higher concentration of Al in the synthesis gel gives a slower crystal growth, which in turn leads to smaller particles. Liu27 and co-workers have shown that both the concentration of SDA and the alkalinity are important parameters that can influence the phase purity and morphology of ZSM-23. The ZSM-23 zeolite is a high silica framewok28 and the Al content can only be adjusted in a narrow range of composition while using the same pH and concentration. Moving outside this range leads to formation of siliceous amorphous species or other crystalline phases that can be formed without the presence of an organic SDA, such as ZSM-517,22,27, mordenite17, and cristobalite16. It should be emphasized that the use of the diquaternary templating agent has the advantage of giving high selectivity for ZSM-23, since the flexible alkane chain fits well into the 1-dimensional channels and the distance between the two terminal nitrogen atoms gives the selectivity for a specific channel system20. That means a lower concentration of the templating agent is permissible and that a much broader range of Si/Al composition can be achieved22.

Results - catalyst performance

The catalyst performance of the 5 materials highlighted here was investigated in the conversion of methanol to hydrocarbons at low feed rates. Previous investigations have shown that higher feed rates, or shorter residence times, do not allow sufficient time for the all-important hydrocarbon pool species to accumulate within the pores29.

Clearly, there is a huge difference in stability and lifetime among the catalysts. This difference is quantified further by the total conversion capacities, defined as the total amount of methanol converted into hydrocarbons until complete deactivation, which are listed in Table 2. Importantly, it seems clear that lifetime is linked to particle dimension, and in particular the dimension in the direction of the channel system. By selecting the appropriate catalyst preparation procedure, the

lifetime can be extended by orders of magnitude. For the material prepared using DMF, the conversion capacity is so small that it might be more appropriate to discuss this as a stoichiometric process between methanol and acid sites. On the other hand, catalysts prepared using the C7 diquaternary SDA always leads to superior catalysts. We have prepared a large number of catalysts using this SDA, and the conversion capacity ranges from 60 up to 170 gmethanol/gcatalyst. However, as the particles become extremely small, reproducibility becomes a major issue, as one might reasonably imagine. Therefore, we have decided to only report data which can be routinely reproduced.

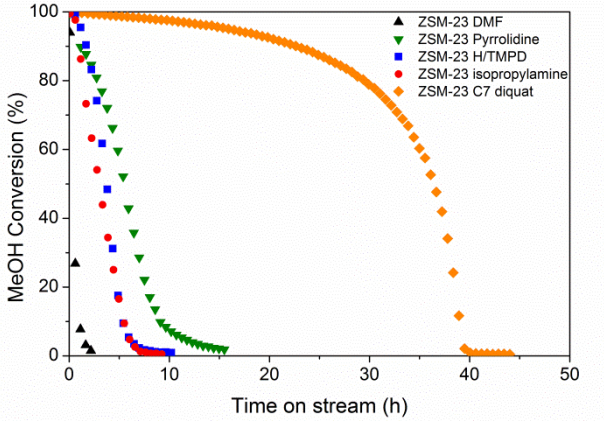

Fig. 2 MeOH conversion over ZSM-23 catalysts at 400 °C, 1 atm and WHSV of 2g MeOH gcatalyst-1 h-1

Previous investigations of ZSM-23 (and the structurally related ZSM-22) report conversion capacities no higher than 16 gg-1 at 400 °C and slightly higher at 450 °C 3,13. Thus, it is clear that the data presented here represent a very significant improvement. For SAPO-34, the archetype MTO catalyst, conversion capacities are typically around 25 gg-1 for commercially relevant catalysts30,31. For ZSM-5, the MTG catalyst, on the other hand, values as high as 1000 gg-1 have been reported32. Nevertheless, the data presented here constitutes a significant step towards the stability required for potential fixed bed application of ZSM-23 in the conversion of methanol to hydrocarbons.

A GC-FID chromatogram of the product distribution at 100% MeOH conversion using ZSM-23 C7 diquaternary as catalyst is presented in Figure 3. As previously reported,3 the quantity of aromatics produced is negligible. Initial data indicate only very subtle differences in product selectivities among the catalysts tested here. Work is currently ongoing to verify and to elucidate the origin of these effects.

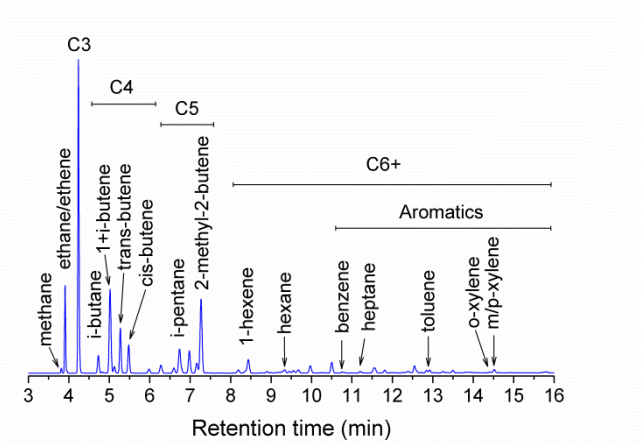

Fig. 3 Gas chromatogram recorded at essentially full methanol conversion for the ZSM-23 C7 diquat. Note the near absence of product peaks in the aromatics region of the chromatogram

Conclusions

Zeolite ZSM-23 catalysts with similar acid density, but widely different particle sizes have been prepared by changing the synthetic parameters and the structure directing agent. Synthesis with pyrrolidine and isopropylamine gives micrometer sized crystals with short lifetime, while the synthesis in presence of an alkyl diammonium salt provides access to very small crystallites, for which the catalytic lifetime increased by at least one order of magnitude. The results indicate that the catalyst lifetime can be explained by the length of the unidirectional channels, which tend to be parallel to the longest crystal dimension, leading to long diffusion pathways and rapid coke accumulation for large crystals.

Acknowledgements

The work is supported by the European Industrial Doctorates project ZeoMorph (FP7 ITN-EID), part of the Marie Curie actions 606965.

Notes and references

1 S. Yurchak, in Studies in Surface Science and Catalysis, ed. C. D. C. D.M. Bibby R. F.Howe and S.Yurchak, Elsevier, 1988, vol. 36, pp. 251–272.

2 J. Topp-Jørgensen, in Studies in Surface Science and Catalysis, ed. C. D. C. D.M. Bibby R. F.Howe and S.Yurchak, Elsevier, 1988, vol. 36, pp. 293–305.

3 S. Teketel, W. Skistad, S. Benard, U. Olsbye, K. P. Lillerud, P. Beato and S. Svelle, ACS Catal., 2012, 2, 26–37.

4 A. Corma and A. Martínez, Catal. Rev., 1993, 35, 483–570.

5 H. Weyda and E. Köhler, Catal. Today, 2003, 81, 51–55.

6 F.-F. Wei, Z.-M. Cui, X.-J. Meng, C.-Y. Cao, F.-S. Xiao and W.-G. Song, ACS Catal., 2014, 4, 529–534.

7 M. Dyballa, U. Obenaus, M. Rosenberger, A. Fischer, H. Jakob, E. Klemm and M. Hunger, Microporous Mesoporous Mater., 2016, 233, 26–30.

8 US4076842 A, 1978.

9 K. Möller and T. Bein, Microporous Mesoporous Mater., 2011, 143, 253–262.

10 K. Y. Lee, H.-J. Chae, S.-Y. Jeong and G. Seo, Appl. Catal. Gen., 2009, 369, 60–66.

11 I. M. Dahl, R. Wendelbo, A. Andersen, D. Akporiaye, H. Mostad and T. Fuglerud, Microporous Mesoporous Mater., 1999, 29, 159–171.

12 I. Pinilla-Herrero, C. Márquez-Álvarez and E. Sastre, Catal. Today, 2016, 277, Part 1, 29–36.

13 H.-G. Jang, H.-K. Min, J. K. Lee, S. B. Hong and G. Seo, Appl. Catal. Gen., 2012, 437–438, 120–130.

14 R. Khare, D. Millar and A. Bhan, J. Catal., 2015, 321, 23–31.

15 J. Wang, S. Xu, J. Li, Y. Zhi, M. Zhang, Y. He, Y. Wei, X. Guo and Z. Liu, RSC Adv., 2015, 5, 88928–88935.

16 B. Wang, Z. Tian, P. Li, L. Wang, Y. Xu, W. Qu, Y. He, H. Ma, Z. Xu and L. Lin, Microporous Mesoporous Mater., 2010, 134, 203–209.

17 Q. Wu, X. Wang, X. Meng, C. Yang, Y. Liu, Y. Jin, Q. Yang and F.-S. Xiao, Microporous Mesoporous Mater., 2014, 186, 106–112.

18 H. J. Lee, S. H. Kim, J. H. Kim, S. J. Park and S. J. Cho, Microporous Mesoporous Mater., 2014, 195, 205–215.

19 S.-H. Lee, C.-H. Shin, D.-K. Yang, S.-D. Ahn, I.-S. Nam and S. B. Hong, Microporous Mesoporous Mater., 2004, 68, 97–104.

20 A. Moini, K. D. Schmitt, E. W. Valyocsik and R. F. Polomski, Zeolites, 1994, 14, 504–511.

21 B. Han, C.-H. Shin, I.-S. Nam and S. B. Hong, in Studies in Surface Science and Catalysis, ed. N. Ž. and P. N. J. Čejka, Elsevier, 2005, vol. 158, Part A, pp. 183–190.

22 S. Ernst, R. Kumar and J. Weitkamp, in Zeolite Synthesis, American Chemical Society, 1989, vol. 398, pp. 560–573.

23 S. Brunauer, P. H. Emmett and E. Teller, J. Am. Chem. Soc., 1938, 60, 309–319.

24 J. Rouquerol, P. Llewellyn and F. Rouquerol, in Studies in Surface Science and Catalysis, ed. F. R.-R. P.L. Llewellyn J.Rouqerol and N.Seaton, Elsevier, 2007, vol. 160, pp. 49–56.

25 A. W. Burton, K. Ong, T. Rea and I. Y. Chan, Microporous Mesoporous Mater., 2009, 117, 75–90.

26 A. W. Burton, S. I. Zones, T. Rea and I. Y. Chan, Microporous Mesoporous Mater., 2010, 132, 54–59.

27 Y. Liu, Z. Wang, Y. Ling, X. Li, Y. Liu and P. Wu, Chin. J. Catal., 2009, 30, 525–530.

28 A. C. Rohrman, R. B. LaPierre, J. L. Schlenker, J. D. Wood, E. W. Valyocsik, M. K. Rubin, J. B. Higgins and W. J. Rohrbaugh, Zeolites, 1985, 5, 352–354.

29 S. Teketel, S. Svelle, K.-P. Lillerud and U. Olsbye, ChemCatChem, 2009, 1, 78–81.

30 R. L. Smith, S. Svelle, P. del Campo, T. Fuglerud, B. Arstad, A. Lind, S. Chavan, M. P. Attfield, D. Akporiaye and M. W. Anderson, Appl. Catal. Gen., 2015, 505, 1–7.

31 F. Bleken, M. Bjørgen, L. Palumbo, S. Bordiga, S. Svelle, K.-P. Lillerud and U. Olsbye, Top. Catal., 2009, 52, 218–228.

32 S. Svelle, L. Sommer, K. Barbera, P. N. R. Vennestrøm, U. Olsbye, K. P. Lillerud, S. Bordiga, Y.-H. Pan and P. Beato, Catal. Today, 2011, 168, 38–47.